Peloton Evolution in Road Cycling Races

Aymane Al Bagdadi[1], Lucas Brokopp[2], Waleed Saati[3], Abhishek Jha[4], and Illia Nikiforov[5]

[6]Department of Mathematics, University of Luxembourg

February 5, 2026

Abstract

This project studies the evolution and stability of a peloton in multi-stage cycling races. Our approach combines aerodynamic modeling, rider power dynamics, fatigue, and statistical analysis. Drafting is described through spacing-dependent drag reduction, linking aerodynamic effects to rider power output and fatigue via critical power. Analysis of large-scale real race data reveals a sharp transition in finishing time gaps, producing a characteristic peloton "shelf" followed by a long-tailed dropped regime. A minimal two-regime synthetic model reproduces these features, showing that aerodynamic drag and fatigue mechanisms are sufficient to explain peloton cohesion and its gradual fragmentation.

1 Introduction

Competitive cycling emerged in the late nineteenth century as improvements in road conditions and bicycle design transformed cycling from a mode of transport into an organized sport. During the 1890s, a number of one-day races appeared across Europe, the most famous being Paris–Roubaix, first held in 1896. In 1903, the Tour de France was inaugurated, a 21-day stage race that has since become the most prestigious event in professional cycling. Following its success, other major tours and one-day classics such as the Giro d'Italia and Vuelta a España were established, forming the foundation of modern competitive road cycling.

Today, cycling competitions span from youth and amateur levels to elite professional categories, encompassing a wide range of race formats. These include time trials (individual or team-based), one-day classics covering distances of up to 280 km, and multistage tours determined by cumulative time. The structure of these competitions reflects the diversity and endurance demands of the sport, where success depends not only on individual strength but also on strategic collaboration within teams and pelotons.

With the growing popularity and commercialization of cycling, the stakes have risen dramatically. Substantial prize money, sponsorships, and technological investments have driven advances in both equipment and race strategy. The modern era of cycling is characterized by rigorous scientific inquiry into aerodynamics, physiology, and group tactics. This has transformed the peloton into a subject of study at the intersection of physics, mathematics, and complex systems science.

A cycling peloton is a collective of riders that move together in close formation to minimize aerodynamic drag and energy expenditure. The coupling between cyclists arises primarily through drafting, which is defined as the aerodynamic shelter created when one cyclist rides in the wake of another. This allows riders to conserve significant amounts of energy, with those in front experiencing the greatest air resistance while those behind benefit from substantial

reductions in drag. Consequently, the peloton exhibits complex spatial and temporal structures, constantly reorganizing as riders rotate, reposition, and respond to environmental and tactical factors throughout a race.

Although the interactions between individual cyclists are simple in principle, the resulting group behavior is remarkably complex as each rider adjusts their position to balance effort, recovery, and race objectives. Such collective behavior shares deep parallels with models from statistical physics and complex systems science, where microscopic interactions lead to macroscopic order and phase transitions.

Research on cycling dynamics has traditionally focused on three main domains: bicycle design and engineering, athletic physiology, and race strategy. However, the collective dynamics of the peloton have received comparatively limited quantitative attention. Foundational work by Kyle (1979) established the aerodynamic benefits of drafting, while subsequent studies by Olds (1998) and others extended these insights to analyze the factors influencing group stability and breakaway success. More recently, the application of complex systems theory to cycling has highlighted the peloton as an archetype of self-organization, sharing properties with other biological collectives such as bird flocks, fish schools, and huddling penguins.

From an aerodynamic perspective, the reduction in drag achieved through drafting is profound. At competitive speeds exceeding 50 km/h, aerodynamic resistance accounts for up to 90% of total resistive forces acting on a cyclist. Early wind tunnel and field experiments demonstrated that trailing cyclists could reduce drag by as much as 30–50%, yet the precise distribution of aerodynamic benefits within large, dense pelotons remains poorly quantified. Computational Fluid Dynamics (CFD) studies have recently begun to map these effects, but a unified mathematical framework capturing both the physical and behavioral coupling among riders remains an open problem.

Advances in wearable technology and on-bike power meters have made professional road cycling one of the most quantitatively monitored endurance sports. As a result, modern performance analysis and race modelling are naturally framed in terms of mechanical power and fatigue, with power-based metrics providing a compact description of riders' physiological limits. These measures are particularly relevant in the peloton, where aerodynamic interactions strongly modulate the power required to maintain race speed and therefore shape the accumulation of fatigue. Understanding how power demand, fatigue, and tactical positioning interact is essential for analysing race dynamics and predicting decisive moments.

In this report, we develop and analyze mathematical models that describe the collective dynamics of a cycling peloton. Our approach integrates the aerodynamic mechanisms that govern peloton formation and race dynamics with physiological models of fatigue that determine a rider's capacity to produce power at critical moments. Finally, we characterize the inherently statistical nature of competitive cycling by working on real data and creating a synthetic data and investigate how external factors influence the outcome of the race.

2 CFD Simulation of the Aerodynamic Phenomena of a Peloton of Cyclists

The fluid dynamics has a very strong impact on the performance of the cyclists in a peloton. To improve energy efficiency and overall performance, air resistance and the suction effect must be minimized.

Two main factors affect the distribution of aerodynamic drag:

- Peloton formation.
- Relative positions of cyclists.

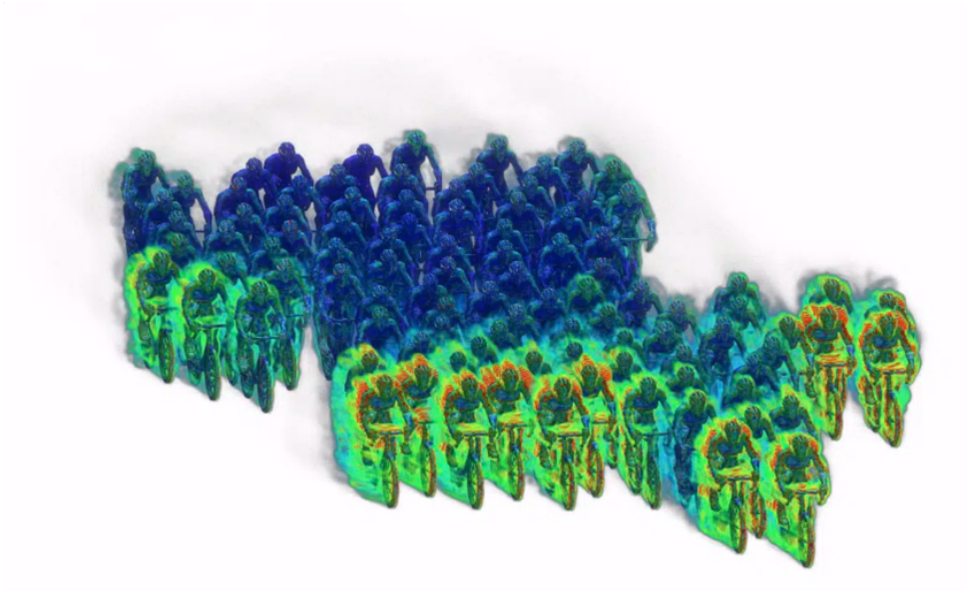

Figure 1: Volumetric field of vorticity around the peloton. Ref: https://eolios.eu/

In the figure above, it is obvious that the cyclist at the front experiences more air resistance than the cyclist behind, and the latter benefits from a significant reduction in drag.

The fluid dynamics around a peloton is a very complex system; therefore, it is difficult to study it empirically since many parameters are involved, including wind speed, wind direction, air humidity, and cyclist position, etc. This is where a mathematical modeling tool such as CFD simulation becomes extremely valuable for studying airflow around the peloton.

CFD simulations help explore different configurations to identify the most effective cyclist positions and peloton formations in terms of drag reduction.

To ensure that the effects of aerodynamic forces are compared accurately, the geometry of each cyclist must be standardized so that the analysis focuses only on the impact of cyclist positions and peloton formations.

This geometric consistency guarantees that any differences observed in aerodynamic forces arise solely from the interactions between the cyclists and their relative positioning, leading to more reliable and meaningful results.

2.1 Aerodynamic Drag: Air Influence on Performance

Aerodynamic drag, or air resistance, is a key factor affecting a cyclist's performance. It arises from the interaction between the rider–bike system and the surrounding air and depends on air density, speed, frontal area, and the drag coefficient, which reflects aerodynamic efficiency.

Since drag increases with air density and with the square of velocity, cyclists effectively push the air in front of them as they move. Lowering air density or minimizing frontal area, such as by adopting a more streamlined, prone position, can substantially reduce drag.

The airflow around the cyclist creates a high-pressure zone in front and a low-pressure wake behind, both contributing to resistance. This wake extends several meters and affects other riders.

In group riding, or within a peloton, positioning plays a major role: cyclists behind others experience reduced drag, especially when riding in single file or close formation, with the effect depending on spacing and posture.

2.2 Velocity and Pressure Distribution Around Cyclists Using CFD Simulation

Computational Fluid Dynamics (CFD) simulations illustrate how airflow velocity and pressure vary around cyclists in a peloton. Because drag force increases with the square of velocity, these simulations help identify the most aerodynamically favorable positions within the group.

At an apparent airspeed of 15 m/s (54 km/h), the lead cyclist experiences the greatest drag, while riders positioned deeper within the peloton face lower relative airspeeds and consequently less resistance.

The horizontal and vertical velocity planes clearly show that front riders act as windbreaks, shielding those behind them and significantly reducing the aerodynamic load on trailing cyclists.

Pressure maps further reveal a "suction effect," where low-pressure zones created behind leading riders decrease the overpressure acting on those following. This effect allows cyclists within the peloton to maintain high speeds with reduced effort.

CFD simulations are valuable for optimizing rider positioning, aerodynamic equipment, and race strategies. In time trials, for instance, they guide athletes in adopting lower, more streamlined postures and in selecting aerodynamic gear such as specialized frames, helmets, and suits. Compared to wind tunnel testing, CFD offers a cost-effective and efficient method to refine aerodynamics, enabling cyclists and teams to minimize drag and improve overall performance.

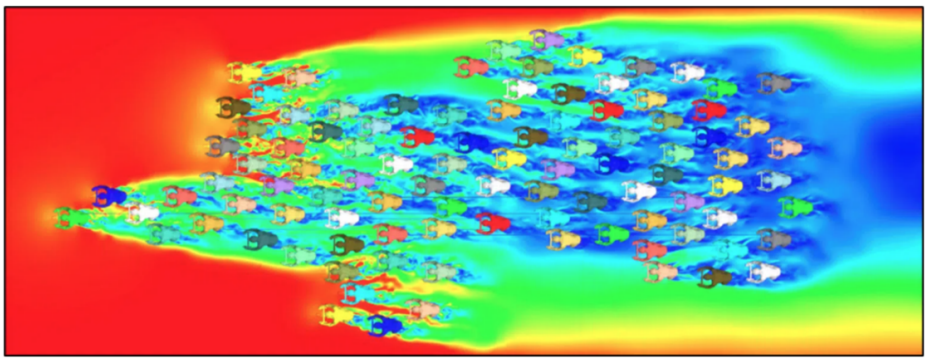

Figure 2: Horizontal plane of speeds within the peloton. Ref: https://eolios.eu/

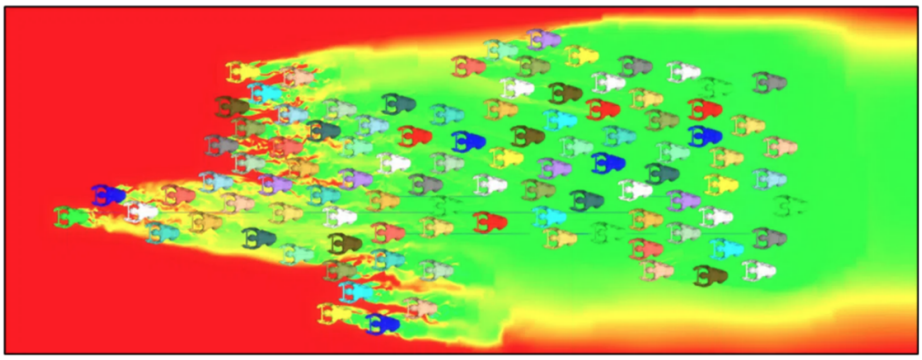

Figure 3: Horizontal pressure plane in the pack. Ref: https://eolios.eu/

2.3 Measuring Drag in CFD Simulation

The CFD analysis quantified the drag forces acting on each cyclist to determine the most aerodynamically favorable positions within the peloton.

The results are expressed as percentages relative to the drag experienced by the lead cyclist, who represents the reference value of 100%.

The drag distribution map highlights that riders positioned deeper in the peloton experience significantly reduced aerodynamic resistance. In particular, cyclists in central positions encounter roughly half the drag of the front rider, demonstrating the substantial protective effect created by surrounding cyclists.

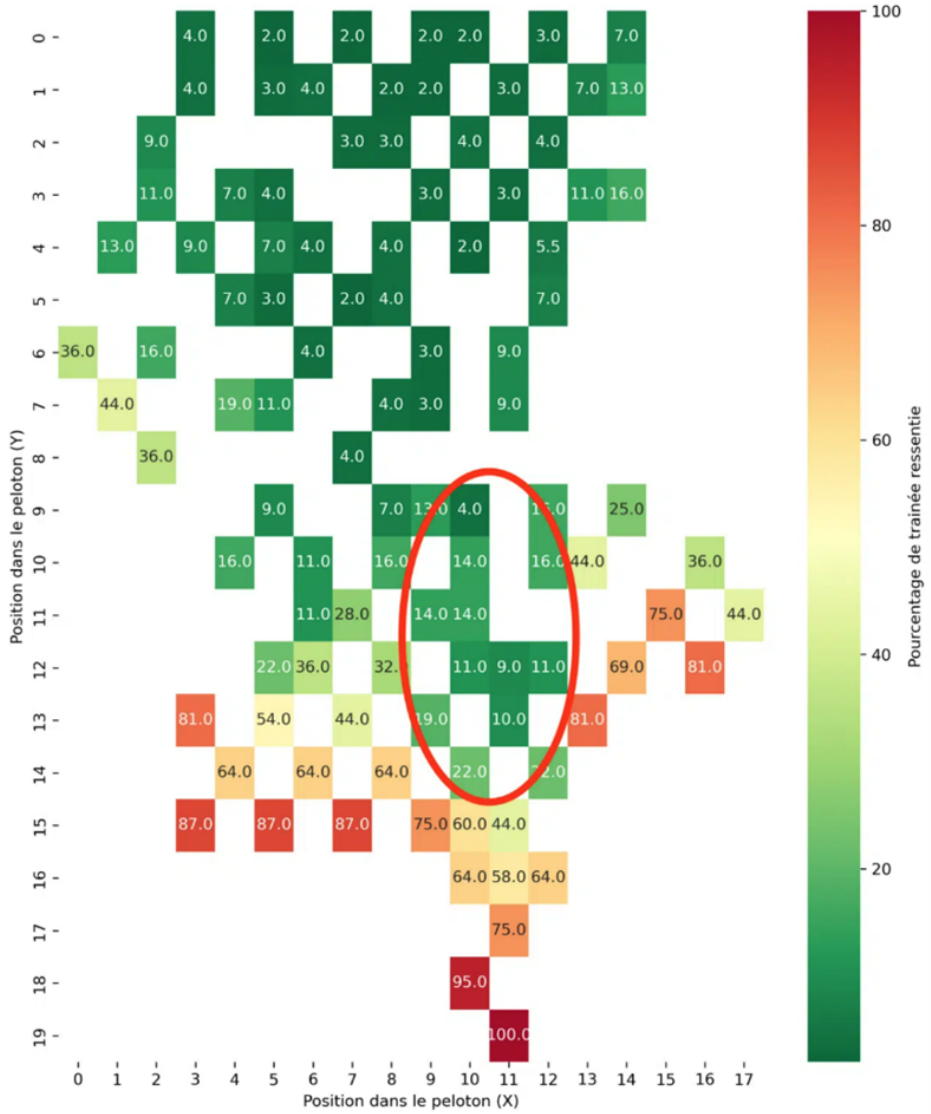

Figure 4: Percentage of drag felt compared to the drag felt by the leader. Ref: https://eolios.eu/

2.4 Cyclist Placement Strategy to Minimize Drag

In general, all cyclists within a peloton experience lower aerodynamic drag than the lead rider. The further a cyclist is positioned toward the rear, the less drag they encounter.

This trend is also evident for riders in the central region of the group, who benefit from reduced air resistance compared to those on the outer edges.

CFD results indicate that the area outlined by the red circle represents the most aerodynamically favorable zone at the beginning of a race. Cyclists in this region experience only about 10–20% of the drag felt by the leader while remaining close to the front of the pack, allowing for significant energy conservation.

However, optimal positioning is not determined by aerodynamics alone. Riders positioned too far back are more susceptible to sudden speed changes (accordion effects) and potential collisions. Consequently, team leaders in events such as the Tour de France often maintain

positions near the front, supported by teammates who balance aerodynamic efficiency with race safety and strategy.

2.5 The Edge Phenomenon in Cycling: Fan Formation as a Strategy Against Crosswinds

When exposed to crosswinds, cyclists adopt a fan (echelon) formation to reduce aerodynamic drag and maintain efficiency.

In this arrangement, each rider positions slightly behind and to the side of the one in front, sheltering from the wind's direct impact. The stronger the crosswind, the further laterally displaced the riders become to maximize protection.

A cyclist left unprotected on the windward side is said to be "in the gutter" (or "kerbed"), facing greatly increased effort to maintain pace.

Single and Double Fan Configurations

Two main fan formations are used depending on group size:

- **Single fan:** Suited for small groups, such as breakaways or team time trials. Riders take turns leading before easing off and rotating back into the sheltered line.
- **Double fan:** More efficient for larger groups, consisting of two rotating lines — one windward (descending line) and one leeward (ascending line). This structure ensures continuous shelter for all riders through coordinated relay rotations.

Tactical Use and Aerodynamic Effects

Forming an effective fan requires at least ten riders.

Teams often exploit this strategy to control positioning and isolate rivals, especially under strong crosswinds.

Riders unable to integrate into the fan face direct wind exposure, a sharp increase in aerodynamic drag, and higher energy expenditure, often leading to splits in the peloton.

CFD Analysis of Fan Formations

A CFD study conducted on an eight-rider double fan formation under crosswind conditions confirmed the aerodynamic advantage of this configuration.

The simulations showed that air velocities around protected cyclists were significantly lower, resulting in a 70% reduction in drag compared to the leading riders.

Specifically, the six sheltered cyclists experienced only about 30% of the total drag felt by the two riders at the front.

Visualization of the volumetric vorticity field revealed that the leading cyclists experienced the greatest airflow disturbance and drag forces, while those in the wake benefited from smoother, slower airflow.

These findings confirm the aerodynamic effectiveness of fan formations in mitigating crosswind effects, conserving energy, and maintaining group cohesion during competitive racing.

3 Spacing and Power Requirements (Illia's part)

Aerodynamic forces play a significant role in cycling when cyclists reach high speeds. When gaining high speeds, the cyclist experiences resistance acting on their bike and their body. This resistance is commonly referred to as aerodynamic drag. When it comes to how much energy an athlete has to exert to continue the race, drag becomes the main factor that affects this. Even small changes in air resistance inevitably lead to noticeable differences in the cyclist's ability to maintain the pace of the race, which, as a result, greatly affects the speed of the peloton, the position of the participants and their fatigue.

In particular, riding close together in a group is one of the main ways to reduce drag. The cyclist who rides first in the group (the lead cyclist) creates an area of lower air pressure behind him, into which the cyclists who follow him fall. The effect that allows a cyclist riding behind another cyclist to save a significant amount of energy is called drafting. Accordingly, the most drag will be experienced by those participants riding on the edges of the peloton, since they are the first to be affected by aerodynamic drag, while the cyclists in the middle of the peloton experience the least drag, because they are protected on all sides by the other participants. Therefore, in order to increase the efficiency of the participants and achieve better results, the peloton tends to compress into a tight shape.

In contrast, models used to analyze energy expenditure and fatigue rely on numerical values.The goal of this part is to develop a mathematical model that describes how cyclist spacing affects aerodynamic drag and, consequently, the power required to maintain speed.

In this section, the focus will be on exploring a mathematical model that relates the physical distance and the aerodynamic drag acting on them to the power the cyclists produce. The model aims to adapt the standard drag equation and introduce a distance-dependent drag coefficient. This will allow us to translate airflow models into a quantitative framework.

3.1 Physical Background: Aerodynamic drag in cycling

What is aerodynamic drag

Aerodynamic drag is the force of resistance that acts on an object as air moves. For example, when a cyclist moves forward, he passes through the air and it pushes back. This force is called drag. In cycling, drag is one of the most important types of resistance. According to Kyle (1979), wind resistance is responsible for most of the metabolic cost of cycling (80-90%).

Pressure drag is created by the difference in air pressure around the cyclist. When moving forward, a high-pressure area is formed in front of the cyclist, while a low-pressure trail is created behind. As a result, the difference between them pulls the cyclist back. It should also be noted that the position of the cyclist's body affects the magnitude of the pressure difference.

In other words, aerodynamic drag is the air's resistance to being displaced. Resistance increases with the cyclist's speed, and even minor details like the shape of the equipment or the cyclist's posture are crucial at the professional level.

Standard drag-force equation

To describe aerodynamic drag mathematically, we will use the standard drag-force equation, which comes from classical fluid dynamics (Martin J., Douglas I. 1998):

$$F_d = \frac{1}{2}\,\rho\, C_d\, A\, v^2.$$

where

- ρ is air density
- C_d is the coefficient of drag

- A is the frontal area
- v is the air velocity tangent to the direction of travel of the bike and rider (which depends on wind velocity and direction as well as the ground velocity of the bicycle).

It is important to mention that drag increases with v^2, therefore a small increase in speed leads to a large increase in resistance. For instance, raising speed from 10 m/s to 12 m/s increase drag by 44%.

This equation gives us an idea that speed is not the only factor that affects drag. Arm and torso positioning or riding behind another rider reduces C_d or A, which reduces the force acting on the cyclist.

In the following sections, this equation will be used to account for the presence of other riders and show how the distance between them affects drag and other factors.

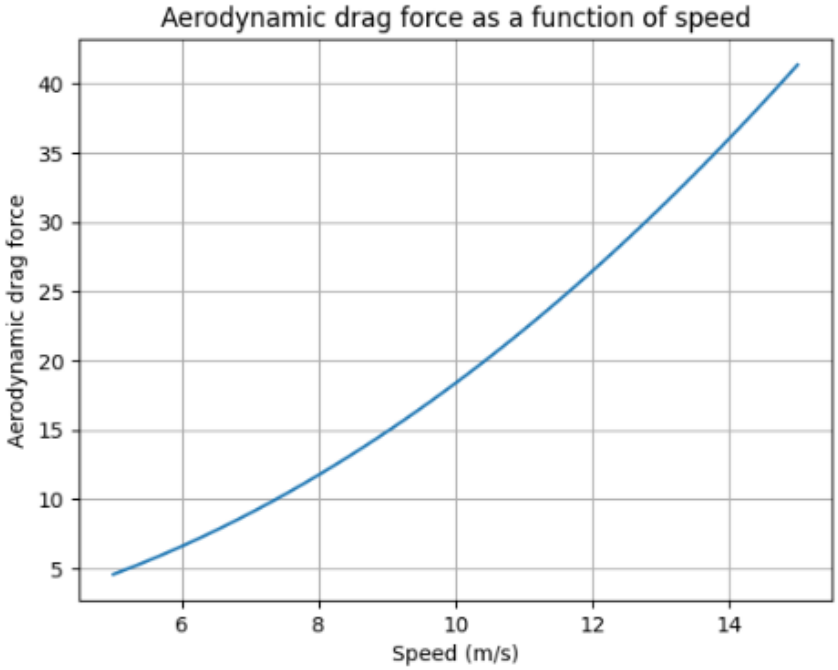

Figure 5: Aerodynamic drag force as a function of speed

This quadratic dependence is shown in Figure 5. The aerodynamic drag force increases as speed rises. This graph explains that maintaining high speed during a race requires significant effort from the cyclist.

Energy cost of maintaining speed

It should be noted that drag also affects how much energy a cyclist needs to produce to maintain a constant speed. Power is the force with which a cyclist works against the forces acting on them. Power is the product of force and velocity.

Power needed to maintain speed can be expressed as:

$$P = F_d \cdot v = \frac{1}{2}\rho C_d A v^3.$$

The cube of the speed ratio shows why cycling at high speeds is physically demanding and why aerodynamic efficiency is valuable.

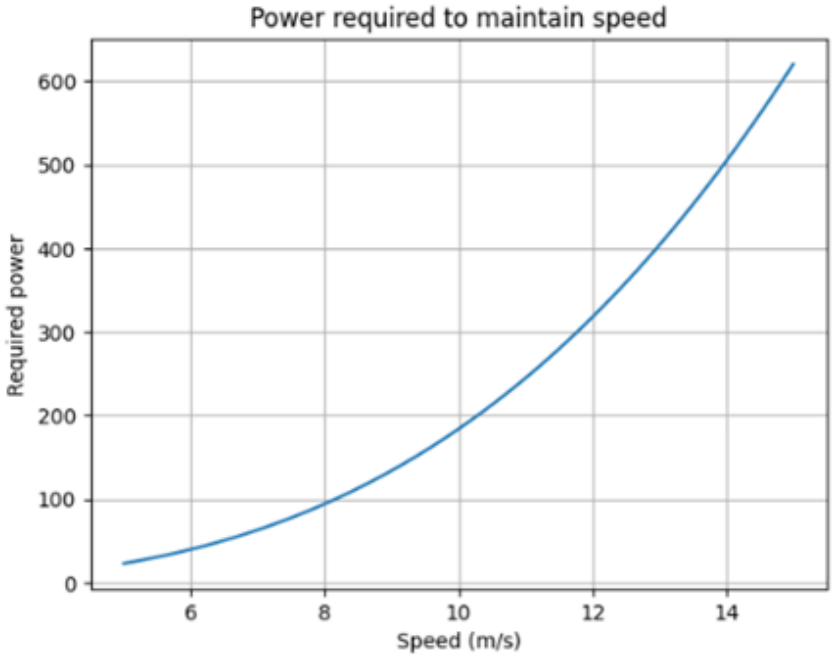

Figure 6: Power required to maintain speed

This cubic relationship is illustrated in Figure 6. The graph shows the relationship between speed and the force required to overcome aerodynamic drag.

In summary, since the required power increases with velocity, reducing drag is one of the most effective strategies for improving cycling efficiency.

3.2 Drafting and Aerodynamic Interactions Between Cyclists

Drafting is the effect that happens when two or more cyclists ride close behind each other to reduce aerodynamic drag. In this case, the cyclist, which goes behind the one in front of him, can benefit from the low pressure area behind the leading cyclist (Blocken B., Druenen T. 2018). The disturbed region of airflow which is created by a leading cyclist is known as wake zone.

A trailing cyclist require less power to follow the race at the same speed. The riders inside the wake zone can save a sufficient amount of energy just by staying within the wake zone. However, the lead cyclist doesn't receive any benefit from that. Also, the effect becomes stronger when the distance between the lead cyclist and the trailing one decreases.

So, riding within a group, especially at high speed, is often much easier and energy-saving compared to riding alone.

Empirical findings

Some of the observations related to drafting were introduced earlier in the project, particularly how pelotons reduce air resistance. As previously noted, early wind-tunnel studies demonstrated that trailing cyclists can reduce drag by approximately 30–50% when positioned directly behind another rider. These findings come from the work of Kyle (1979).

According to the Kyle's experiment, the closer the trailing rider is to the leader, the more advantage they can gain from drafting.

Later work by Olds (1998) expanded these observations to larger groups. His results showed:

- **Single** Trailing cyclists experience approximately 30–50% drag reduction,

- **Two-rider** The trailing cyclists experiences a major benefit. Each next rider reduces drag more for those who are behind them. In other words, the further away from the leader you are, the less effective you become in the chain of cyclists.
- **Peloton** Cyclists in the middle of a peloton are surrounded by colleagues on all sides, so they may benefit from bigger reductions in drag. The drag can drop up to 20% of the drag which the lead cyclist experiences.

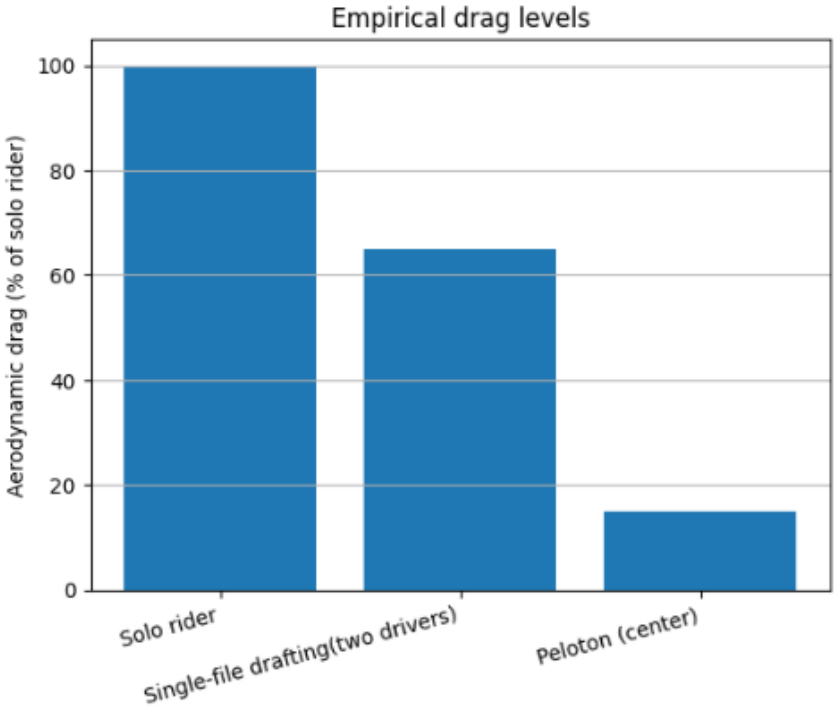

Figure 7: Power required to maintain speed

As already mentioned earlier in the report, empirical studies show drag reductions for riders who draft behind others. Figure 7 summarizes typical drag levels of a solo rider, two riders, and riders inside a peloton.

These results show how the cyclists' position affects the resistance they experience.

The role of spacing

The distance between cyclists plays a key role in how much drag is reduced by movement. Since the wake behind cyclists is not uniform, its size changes with distance. The strongest part of the wake is located up to 30 centimeters away, so the cyclist riding very close behind experiences the largest reduction in drag. Very small changes in spacing can produce surprisingly large differences in drag.

For example, even changing the distance between riders from 30 to 60 centimeters can significantly increase drag. A change of more than 2 meters means that drafting becomes minimal.

In this regard, riders try to stay as close as possible to maximize aerodynamic savings, while not approaching too close for safety reasons. In the following sections, this relationship will be shown using a mathematical formula to build a model.

3.3 Mathematical Modeling of Drag Reduction as a Function of Spacing

Why we need a spacing-based drag model

Aerodynamic interactions often change over time as cyclists adjust their distance from each other. Even small variations in the distance between them can cause noticeable changes in drag and power requirements. The purpose of this section is to lay the foundation for building an analytical model of how drag changes as a function of spacing.

Classical drafting correction factor (Olds, 1998)

In order to model drafting effects we can express the drag force as a fraction of the drag they would experience when riding alone. Let $F_{d,\text{solo}}$ denote the aerodynamic drag force for a solo rider. When drafting, the effective drag can be written as

$$F_d(s) = F_{d,\text{solo}} \cdot CF_{\text{draft}}(s).$$

where

- s - spacing between cyclists
- $CF_{\text{draft}}(s)$ - drafting correction factor,

$$0 < CF_{\text{draft}}(s) \leq 1$$

- $F_{d,\text{solo}}$ - aerodynamic drag (solo rider)

According to the research, Olds (1998) proposed emperical polinomial to the $CF_{\text{draft}}(s)$:

$$CF_{\text{draft}}(s) = 0.62 - 0.0104\, s + 0.0452\, s^2.$$

with s measured in meters. For spacings larger than 3 m, the drafting effect vanishes and $CF_{\text{draft}} = 1$.

It provides a description of how aerodynamic resistance depends on distance in the case when cyclists move in one lane.

Smooth spacing-based drag model

The polynomial expression given in the previous subsection is based on experimental data and does not generalize to peloton configurations. So it is useful to introduce a smooth function that shows the change in draft efficiency with increasing distance.

The dependence of drag reduction on spacing can be approximated by an exponential function:

$$f(s) = a + (1 - a)e^{-bs}$$

In this formula a and b are positive parameters that control the drag level and the rate at which its effectiveness decreases with distance.

It satisfies the limits:

$$f(0) = a, \qquad \lim_{s\to\infty} f(s) = 1.$$

This form provides a simple approximation that reproduces qualitative behavior: 1) Small spacing leads to strong drug reduction; 2) Large spacing leads to small drug reduction.

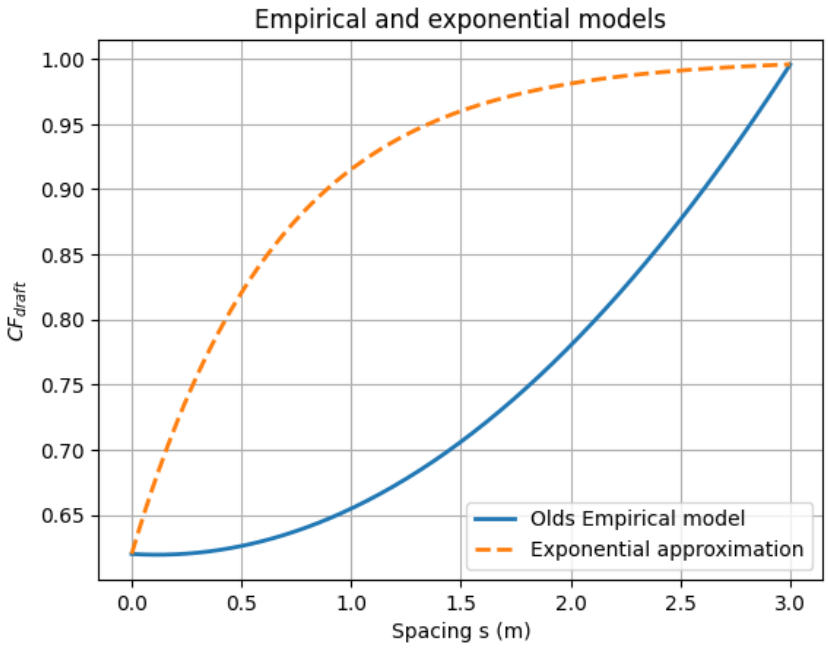

Figure 8: Empirical and exponential models

The figure shows how aerodynamic drag increases as cyclists move farther apart. The exponential model provides a smooth approximation of the empirical data.

Relation between peloton density and spacing

We can introduce a measure of peloton density in order to relate individual spacing to the spacing in pelotons:

$$D = \frac{N}{A},$$

- N - number of cyclists
- A - effective cross-sectional area occupied by the peloton

The average distance between cyclists scales inversely with the square root of density, in case we assume a uniform distribution of cyclists:

$$s \propto \frac{1}{\sqrt{D}}.$$

This relation captures the idea that denser pelotons correspond to smaller rider distances.

Final drag and power model

Now we can write an expression for the power required to maintain a given speed:

$$P(s) = \frac{1}{2}\,\rho\, C_d\, A\, v^3\, f(s),$$

where

- ρ is air density
- C_d is the coefficient of drag

- A is the frontal area
- v is the air velocity tangent to the direction of travel of the bike and rider (which depends on wind velocity and direction as well as the ground velocity of the bicycle).
- $f(s)$ drafting effects due to spacing

This model links aerodynamic drag, power expenditure, and cyclist spacing. It will be used for the numerical simulations used in the next section.

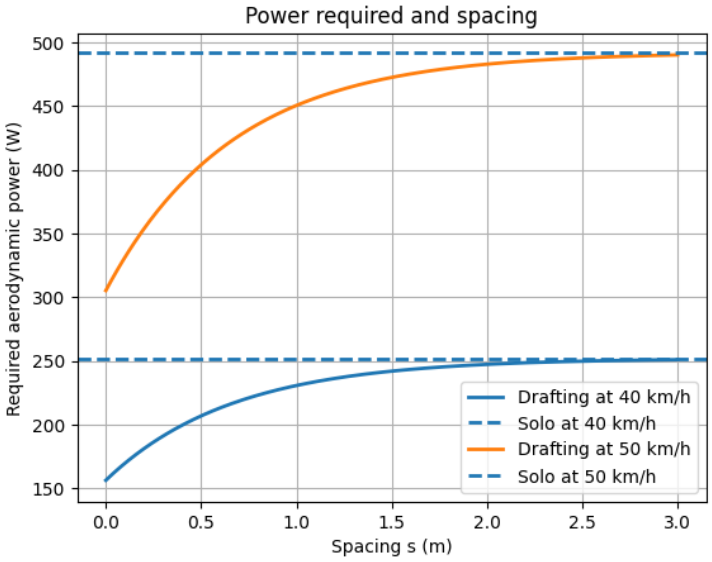

Figure 9: Power required and spacing

As spacing increases, drafting benefits diminish and the required power approaches solo riding conditions.

3.4 Power Savings from Drafting

Definition of power savings

Using the model from the previous section, we can quantify the energetic benefit of drafting in a simple way. The power savings can be defined as the difference between the power required to maintain speed for solo rider and the power required for cyclists in peloton at spacing s:

$$\Delta P(s) = P_{\text{solo}} - P(s).$$

- P_{solo} is the aerodynamic power required for solo rider
- $P(s)$ is the power required for cyclists in peloton at spacing s

A positive value of $\Delta P(s)$ is the amount of power saved due to reduced aerodynamic drag. This definition allows us to compare different peloton positions using one quantitative measure.

The energy savings in this this context can be linked to fatigue development.

Energy savings at different peloton positions

We can now show the energetic benefit of drafting for common positions in peloton. It can be done by using the power model from the previous section and the definition of energy savings that we just gave.

Let's consider three characteristic positions:

- Rider that goes behind the leader with minimal spacing (s = 0.3 m)
- Rider who is located in the middle of peloton with slight larger spacing (s = 0.7 m)
- Rider in the back of peloton, the spacing is large (s = 1.5 m)

In this part we stop talking about positions in the abstract and link the model to real positions in the peloton. Each position has its own spacing which increases with distance from the leader. This can be shown that the energy savings vary depending on the cyclist's position and their speed.

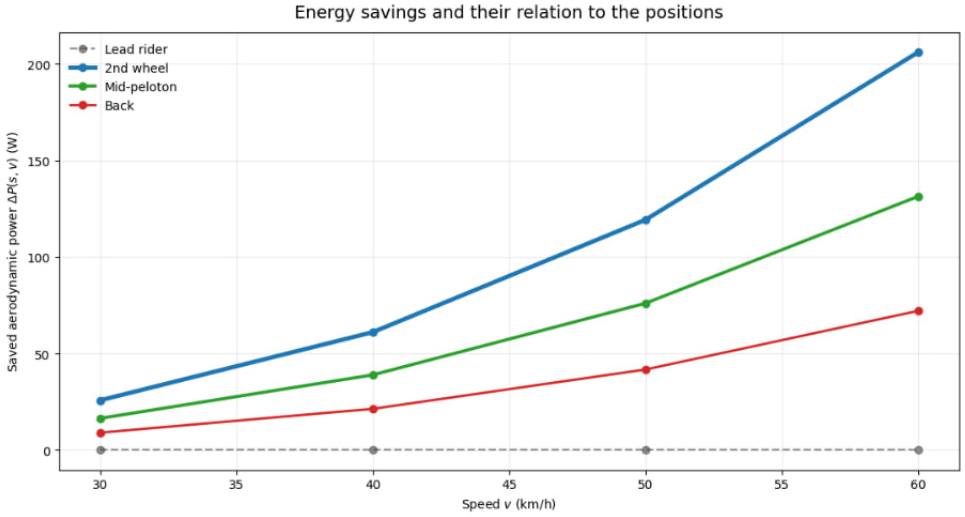

The provided graph shows how both speed and position of cyclists in the peloton affect saved aerodynamic power. As we can see, the lider, in fact, gains no benefit, however riders at the back of the peloton experience significant profit in required power. The cyclists in the mid-peloton and the 2nd wheel position benefit the most, the latter might save more than 200 W from draftin at high speed.

I will note that as speed increases, the distance between the curves also increases, which means that at high speeds even a slight change in position can lead to significant changes in power savings.

This figure clearly shows that positions behind the leader allow us to save more energy, or the greater the distance from the leader, the less energy we save, regardless of speed. This explains why cyclists always try to be as close as possible to the leader of the race.

3.5 Simulations and Graphical Results

The purpose of this section is to present the mathematical and analytical results obtained in the previous sections in the form of visual interpretations. We have already explained theoretically which formulas were used and how they affect the model, now we need to show how they work in the form of race conditions.

The graphs presented in this section have been specially designed to show the dependence of spacing, energy savings due to drafting and cyclists' speed.

The graphs are intended to show how to quantify spacing and power savings at different speeds, as well as to compare factors such as modes and energy hierarchies.

Instead of focusing on a single curve, the comparative behavior of the curves and uncertainties has been considered.

Saved aerodynamic power from drafting vs spacing

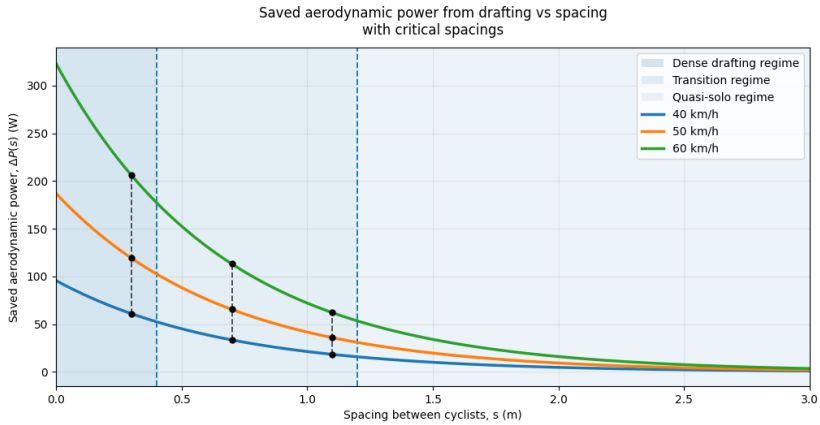

Extracted values of ΔP (W) at critical spacings

	40 km/h	50 km/h	60 km/h	Avg. ΔP
s = 0.3 m	61.1	119.3	206.1	72.5
s = 0.7 m	33.5	65.5	113.1	39.8
s = 1.1 m	18.4	35.9	62.1	21.8

The given figure shows the relation between saved power and spacing which was obtained using this formula:

$$\Delta P(s) = P_{\text{solo}} - P(s).$$

for speeds 40, 50, and 60 km/h.

The vertical dashed lines were added to the graph in order to divide the plot into 3 parts:

- Dense drafting regime (small spacing)
- Transition regime (medium spacing),
- Quasi-solo regime (large spacing)

The critical points are highlighted by black color. These points are the ones that were taken for the table to present quantitative comparisons.

This gives us an understanding that drafting effectiveness is strictly regime dependent rather than simply continuous. The figure shows that small changes in spacing lead to large energy changes.

As a supplement to the graph, a table with numerical values of the critical points was provided. This was done so that we could numerically compare how much power savings increase with speed under the same spacing conditions.

The table shows the values of the critical points in watts, and also emphasizes how much each 10 additional kilometers in speed affects power saving. Based on the results of the table, we can emphasize that drafting is strategically critical.

Saved power vs spacing with uncertainty Monte Carlo

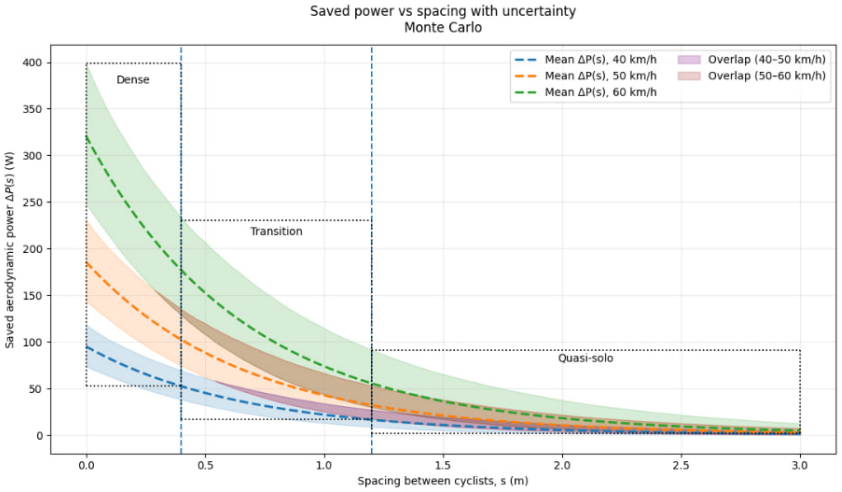

This figure introduces an uncertainty parameter into the model, as the force required to maintain velocity is not a constant value and can vary depending on parameters such as drafting strength, and decay rate. For each velocity, a semi-transparent range is presented with a 5-95 percentile value of the saved power obtained using Monte Carlo. Overlappings of these semi-transperent regions are highlighted.

The figure also shows dotted rectangles for each of the three regimes, showing the area of potential power savings depending on the speed and uncertainties. They show the main difference in drafting effectiveness between the regimes: for example, dense and high in the dense regime and very little in the quasi-solo.

Application of the Model to Real Race Data (Illustrative Example)

As an addition to the previous simulations, we present a model that shows the spacing-data framework and how it can be displayed on race data. The purpose of this figure is to test the consequences of the model configuration based on a real peloton.

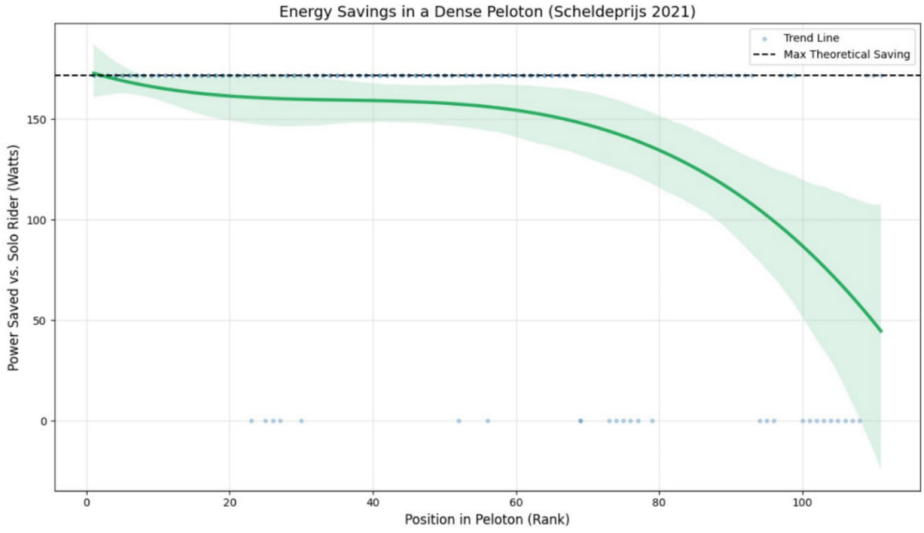

These observations are consistent with the simulation results. In particular, one can notice the existence of a dense regime with transition to transition and quasi-solo conditions, reflecting the gradual disappearance of the drafting effect. This observation confirms the quality of the conclusions of the main two simulations.

The figure shows the relationship between power saving and driver position in the Scheldeprijs 2021 race. The aerodynamic power saving in this problem is found using the same functional relationship as in the previous sections. The line sections, with standardized aerodynamic parameters. A reference "maximum theoretical saving" is given to indicate the upper limit imposed by the drafting model.

It should be noted that the purpose of this figure is to illustrate, not to verify.

4 Fatigue Development and Power Dynamics in the Peloton

To model fatigue development within a cycling peloton and its influence on race outcomes, it is essential to characterize the underlying physical output of cyclists, which is naturally expressed in terms of mechanical power. Advances in wearable technology and on-bike power meters have transformed professional road cycling into one of the most quantitatively monitored endurance sports, enabling detailed physiological modelling of rider performance under race conditions. Modern training analysis and race modelling therefore rely heavily on power-based metrics that quantify sustainable effort, fatigue resistance, and metabolic limits.

A central reference point within this framework is the functional threshold power (FTP), operationally defined as the highest power output a rider can sustain for approximately one hour. FTP serves as a practical benchmark for pacing strategies and the delineation of training intensity zones. Closely related is the critical power (CP) concept, which provides a formal mathematical description of endurance capacity through the relationship between power output and time to exhaustion. Critical power represents the maximal steady-state intensity at which metabolic equilibrium can be maintained. Power produced above CP draws upon a finite anaerobic work capacity, denoted W', while work performed below CP permits partial recovery of this reserve. Together, FTP, CP, and W' provide a compact representation of a rider's ability to tolerate repeated surges, recover between efforts, and deliver decisive power late in a race.

Road cycling races can thus be viewed as long stochastic sequences dominated by low-to-moderate intensity riding interspersed with short, high-intensity surges. Importantly, fatigue accumulation is highly nonlinear with respect to exercise intensity: work performed near and above FTP (or equivalently CP) contributes disproportionately to subsequent performance degradation through accelerated depletion of W' and durability loss. As a result, a practical and widely adopted framework for representing rider workload is the classification of power output into training zones defined as percentages of FTP.

Power output is commonly categorized into seven zones (Z1–Z7). The lower-intensity domains (Z1–Z3) are associated with so-called low-intensity fatigue, which is primarily driven by glycogen depletion, gradual metabolic drift, and shifts in substrate utilization. Empirical findings reported by [1] demonstrate that as race duration increases, fat oxidation progressively rises while the capacity to sustain high lactate-supported power decreases. These lower zones can be maintained for extended durations, with well-trained professional riders capable of sustaining upper Z3 efforts for approximately four hours under race conditions [4].
In contrast, the higher zones (Z4–Z7) correspond to intensities at or above FTP/CP and are associated with high-intensity fatigue. These efforts induce rapid physiological stress through lactate accumulation, phosphocreatine depletion, and neuromuscular fatigue, leading to accelerated depletion of the finite W' reservoir. Recent research indicates that cumulative work performed above threshold is the strongest predictor of a rider's subsequent decline in sustainable power output. Although riders spend relatively little total time in these high zones, their contribution to fatigue development is disproportionately large.

Stage-race data further support this observation: the majority of race time is spent in Z1–Z3, while Z4–Z7 account for a small fraction of total duration yet play a decisive role in shaping race dynamics and performance outcomes [2]. This distribution is illustrated in Figure 10, which highlights the strong asymmetry between time spent and physiological cost across intensity domains.

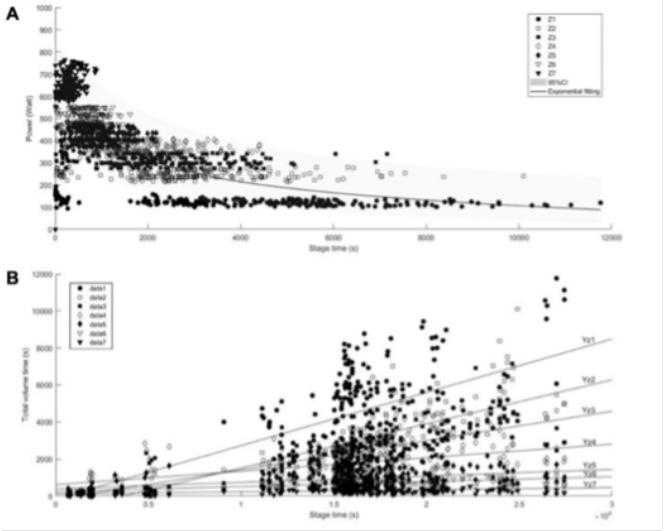

Figure 10: Changes in performance and physiological response across time.

Single-race experimental studies conducted in [7] reveal distinct fatigue signatures across power systems. Peak sprint power declines early in the race and then stabilizes, whereas aerobic performance in the Z4–Z6 range exhibits a gradual reduction over the full six-hour duration, with substantial inter-individual variability (2–14% loss). These observations motivate a two-component fatigue structure: a short-term high-intensity depletion process governing attack and sprint repeatability, and a slower durability decay that accumulates over hours and becomes the primary determinant of late-race performance separation. This is shown in Figure 11 below

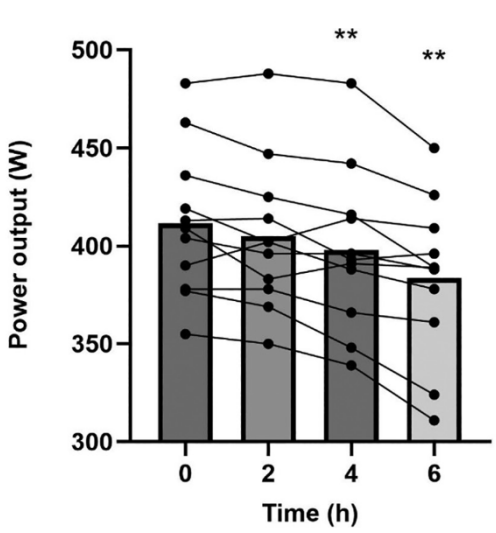

(a) Mean (bars) and individual participants (dots) power output during the 5 km time trial performance test after 0, 2, 4, and 6 h of race simulation.

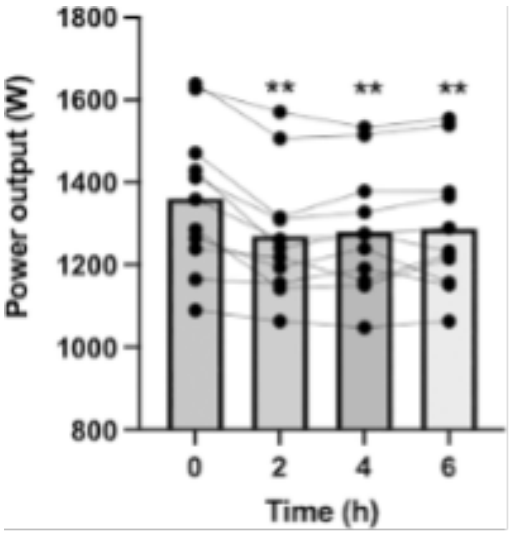

(b) Peak sprint power during the field tests. Mean (bars) and individual (symbols) peak power output accessed during the 100m sprint performance test after 0, 2, 4, and 6 h of race simulation.

Figure 11: Changes in performance and physiological response across time.

Given that fatigue accumulation is dominated by work performed near and above CP, riders actively attempt to minimize unnecessary exposure to high-intensity zones. One of the most effective mechanisms for achieving this is sheltering within the peloton. Drafting substantially reduces aerodynamic drag, allowing riders to maintain race speed at significantly lower mechanical power outputs. This directly reduces the rate of W' depletion and slows the long-term decay of sustainable power.

This mechanism highlights the central importance of team tactics in professional road racing. Domestique riders are strategically deployed to protect team leaders by controlling pace, closing gaps, and positioning the leader within the energetically optimal regions of the peloton. As a result, the leader's fatigue trajectory in terms of cumulative work above CP and long-term durability loss is systematically lower than that of riders exposed at the front or riding in isolation. Domestiques, in contrast, accumulate a disproportionate share of Z4–Z5 workload while performing these duties, effectively sacrificing their own W' and endurance capacity. This redistribution of energetic cost preserves the leader's high-intensity reserve for decisive race phases [8].

The competitive implications of this dynamic become most apparent in the final phase of races. Riders who have accumulated less fatigue either through team protection or superior physiological durability are more likely to successfully initiate or respond to decisive attacks. Simulation results in [1] illustrate this divergence clearly: while some riders exhibit minimal end-of-race performance degradation, others experience time-trial power losses exceeding 10%, with variance increasing as race duration progresses. Protected leaders typically retain access to their high-intensity "reserve," enabling short-duration efforts exceeding 800 W in the closing kilometers, while heavily burdened domestiques experience reductions in both critical power and anaerobic capacity [9].

Environmental conditions further modulate fatigue development by altering the power required to maintain race position and speed. Wind direction plays a dominant role: headwinds

amplify drafting benefits and increase the cost of riding exposed, whereas crosswinds reduce sheltering effectiveness and force riders into higher sustained power outputs, accelerating fatigue accumulation. Terrain exerts an equally important influence. On climbs, aerodynamic effects diminish and gravitational resistance dominates, making fatigue primarily dependent on power-to-weight ratio and sustained high-zone tolerance. This explains the consistent advantage of lighter riders in mountainous stage races. Finally, adverse weather conditions such as rain increase rolling resistance and technical difficulty, leading to greater braking, acceleration, and stochastic surges in power output, all of which intensify physiological load and accelerate fatigue development.

By integrating power-based physiological metrics (FTP, CP, and W'), tactical positioning within the peloton, and environmental forcing, it becomes possible to construct a mathematical framework capable of modelling fatigue evolution and predicting a rider's capacity to generate decisive power in the later stages of a race.

4.1 Fatigue development model for road cycling race dynamics

We model fatigue development in a road cycling race using a hybrid framework that couples (i) a mechanical power demand model driven by race conditions and rider positioning, and (ii) physiological state dynamics capturing both long-term durability loss and short-term high-intensity capacity depletion/reconstitution. The model is simulated in discrete time with step size Δt.

4.1.1 State variables and parameters

For each rider i, we define the following state variables:

$$CP_i(t) \quad \text{current (effective) critical power (W)}, \tag{1}$$
$$W_i'(t) \quad \text{anaerobic work capacity balance (J)}, \tag{2}$$
$$\mathcal{W}_i(t) \quad \text{accumulated mechanical work (kJ)}. \tag{3}$$

The corresponding rider-specific parameters are:

$$CP_{i,0} \quad \text{fresh critical power (W)}, \tag{4}$$
$$W'_{i,\max} \quad \text{maximal anaerobic work capacity (J)}, \tag{5}$$
$$\lambda_i \quad \text{fatigue-resistance parameter controlling durability decay}, \tag{6}$$
$$\phi_i \quad \text{W' recovery efficiency constant}. \tag{7}$$

Environmental stress is represented by a multiplicative factor $R(t) \geq 1$ (e.g. rain), and aerodynamic shelter is represented by a binary drafting indicator $d_i(t) \in \{0, 1\}$ (1 = drafting/sheltered, 0 = exposed).

4.1.2 Mechanical power demand model

At each time step, the mechanical power required to maintain the race speed $v(t)$ on a road of gradient $s(t)$ (in %) under wind $w(t)$ (m/s) is computed from a force-balance model:

$$P_i(t) = \big(F_g(t) + F_r(t) + F_a(t)\big)\, v(t), \tag{8}$$

where F_g is the gravitational component, F_r rolling resistance, and F_a aerodynamic drag.

Gravitational force. Using $s(t)$ as percentage slope, we approximate $\sin(\theta) \approx s(t)/100$:

$$F_g(t) = mg\frac{s(t)}{100}, \tag{9}$$

with total mass $m = m_{\text{rider}} + m_{\text{bike}}$ and gravitational acceleration $g = 9.81$ m/s^2.

Rolling resistance.

$$F_r(t) = mgC_{rr}, \tag{10}$$

where C_{rr} is the coefficient of rolling resistance which is determined by the type of tire that the riders use as well as the surface ridden on.

Aerodynamic drag and drafting. Let $v_{\text{air}}(t) = v(t) + w(t)$ denote the relative air speed (positive for headwind). Aerodynamic drag is modeled as

$$F_a(t) = \frac{1}{2}\rho\, C_d A_i(t)\, v_{\text{air}}(t)^3, \tag{11}$$

with air density ρ and effective drag area $C_dA_i(t)$. Drafting reduces effective drag area:

$$C_dA_i(t) = \begin{cases} C_dA_0, & d_i(t) = 0 \quad \text{(exposed)} \\ \kappa\, C_dA_0, & d_i(t) = 1 \quad \text{(drafting)} \end{cases} \tag{12}$$

where $\kappa \in (0, 1)$ is a drafting reduction factor (e.g. $\kappa = 0.65$ corresponds to a 35% reduction).

4.1.3 Accumulated mechanical work

Mechanical work is accumulated as

$$\mathcal{W}_i(t + \Delta t) = \mathcal{W}_i(t) + \frac{P_i(t)\Delta t}{1000}, \tag{13}$$

where $P_i(t)$ is in watts (J/s), Δt in seconds, and $\mathcal{W}_i$ in kJ.

4.1.4 Long-term fatigue: durability-driven critical power decay

Long-term fatigue, also referred to as durability loss, is modeled as a progressive reduction in the rider's effective critical power due to the accumulation of mechanical work over the race. Rather than assuming linear decay, we adopt an exponential formulation to reflect the nonlinear nature of prolonged physiological stress accumulation observed in endurance exercise.

The effective critical power of rider i at time t is given by

$$CP_i(t) = \max\big(\underline{CP}_i,\ CP_{i,0}\exp\big(-\lambda_i\,\mathcal{W}_i(t)\big)\big), \tag{14}$$

where $CP_{i,0}$ denotes the fresh critical power, $\mathcal{W}_i(t)$ is the accumulated mechanical work (in kJ), λ_i is a rider-specific fatigue resistance parameter. The term $\underline{CP}_i$ imposes a physiological lower bound on sustainable aerobic power output and is set here to $\underline{CP}_i = 0.5\,CP_{i,0}$.

This formulation captures the empirical observation that durability loss accelerates with prolonged high workload exposure, while riders with greater fatigue resistance (smaller λ_i) preserve a higher fraction of their aerobic capacity late in the race.

4.1.5 Short-term fatigue: W' balance dynamics

Short-term high-intensity fatigue is modeled using the W' balance framework, which represents the finite anaerobic work capacity available above critical power. When instantaneous power output exceeds the current critical power, W' is depleted at a rate proportional to the power surplus:

$$W_i'(t+\Delta t) = W_i'(t) - \big(P_i(t) - CP_i(t)\big)\Delta t, \qquad \text{if } P_i(t) > CP_i(t). \tag{15}$$

When power output falls below critical power, W' is reconstituted according to exponential recovery kinetics toward the maximal anaerobic capacity $W'_{i,\max}$:

$$W_i'(t+\Delta t) = W'_{i,\max} - \big(W'_{i,\max} - W_i'(t)\big)\exp\!\left(-\frac{\Delta t}{\tau_i(t)}\right), \qquad \text{if } P_i(t) < CP_i(t), \tag{16}$$

where $\tau_i(t)$ denotes a time-varying recovery constant controlling the speed of W' reconstitution. The recovery timescale is modeled as intensity dependent:

$$\tau_i(t) = \mathrm{clip}\left(\tau_{0,i}\frac{CP_i(t)}{CP_i(t) - P_i(t)},\ \tau_{\min},\ \tau_{\max}\right), \tag{17}$$

where $\tau_{0,i}$ is a baseline recovery parameter and the clipping bounds $\tau_{\min}$ and $\tau_{\max}$ prevent unrealistically fast or slow recovery dynamics.

Finally, physical bounds are enforced on the anaerobic reserve:

$$W_i'(t) \in [0, W'_{i,\max}]. \tag{18}$$

Together, the durability-driven critical power decay and the dynamic W' balance model allow the framework to capture both slow cumulative fatigue processes and rapid high-intensity depletion and recovery cycles that occur during tactical race situations such as climbs, attacks, and drafting phases.

4.1.6 Tactical exposure (drafting) and roles

Using the aforementioned formulas it is possible to create a simulation of a race where we can highlight 3 types of riders, Breakaway rider, domestique, and the leader who is protected from the wind by the domestiques and the rest of the peloton. This helps us understand how based on the power output the fatigue increases and thus the critical power decreases. Given time series inputs $(v(t), s(t), w(t), d_i(t))$ and rider parameters $(CP_{i,0}, W'_{i,\max}, \lambda_i, \phi_i)$, we iterate (8)–(18) forward in time at resolution Δt to obtain trajectories of power output, effective $CP_i(t)$, and W' balance $W_i'(t)$. These outputs summarize fatigue development over the race and can be used to compare riders under different tactical and environmental scenarios. Below we can see a figure which shows this simulation for a flat race and for a mountainous race.

Tactics are represented through time-varying drafting status $d_i(t)$: protected leaders satisfy $d_i(t) \approx 1$ for most of the race, domestiques are exposed ($d_i(t) = 0$) when performing workload at the front and sheltered otherwise, and breakaway riders are typically exposed ($d_i(t) = 0$). Since drafting modifies $C_d A_i(t)$, it directly alters the mechanical power demand in (8) and thereby affects both durability decay (14) via accumulated work (13) and W' dynamics (15)–(16).

By combining tactical positioning, environmental forcing, and physiological fatigue dynamics, the model enables forward simulation of race evolution under realistic conditions. In particular, the framework allows three characteristic rider archetypes to be represented: a protected leader,

whose energy expenditure is minimized through aerodynamic shelter; a domestique, who absorbs workload on behalf of the team and therefore experiences accelerated fatigue accumulation; and a breakaway rider, who remains largely exposed and must sustain high mechanical output for prolonged periods.

Given time-series inputs describing race conditions and course topology, $(v(t), s(t), w(t), d_i(t))$, together with rider-specific physiological parameters $(CP_{i,0}, W'_{i,\max}, \lambda_i, \tau_{0,i})$, equations (8)–(18) are iterated forward in time at resolution Δt to generate trajectories of power output, effective critical power $CP_i(t)$, and anaerobic reserve $W'_i(t)$. These state trajectories describe the evolving energetic capacity of each rider throughout the race.

Crucially, these outputs provide a mechanistic link between tactical decisions, terrain-induced workload, and performance potential in the decisive phases of the race. Riders who preserve higher effective critical power and W' balance late in the race retain a greater ability to initiate or respond to attacks, sustain high climbing power, and produce decisive efforts in final selections or sprints. As such, the model does not only reproduce fatigue development, but also provides a quantitative framework for assessing which riders are most likely to remain competitive as the race progresses. Figure 12 illustrates the resulting fatigue dynamics for two contrasting race scenarios: a flat course dominated by aerodynamic workload and drafting effects, and a mountainous course characterized by repeated long climbing efforts. Together, these simulations demonstrate how course topology and team tactics shape the structure of fatigue development and, in turn, influence the competitive hierarchy within the peloton and the likely outcome of the race.

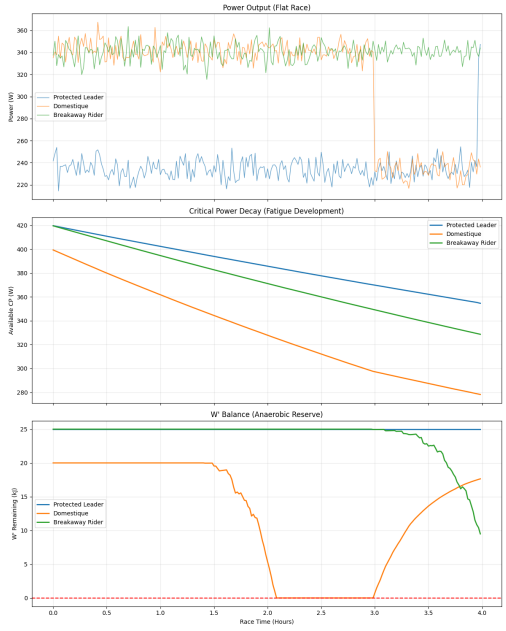

(a) Flat course scenario

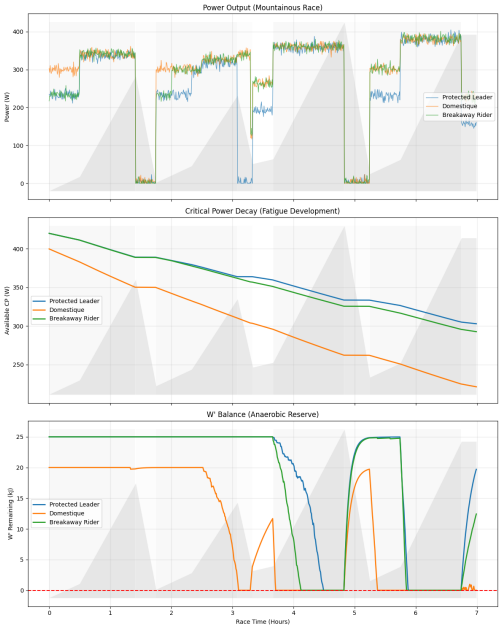

(b) Mountain course scenario

Figure 12: Simulated fatigue development in flat (a) and mountainous (b) race scenarios. In the flat case, power output remains relatively stable and durability fatigue accumulates gradually, with protected riders preserving higher effective critical power and anaerobic reserves due to aerodynamic shelter. In contrast, the mountainous scenario exhibits terrain-driven power plateaus during climbs and recovery phases on descents, resulting in stepwise declines in effective critical power and repeated depletion–reconstitution cycles of W'.

5 Statistical analysis of Peloton finishing times

In this section, we analyse the statistical structure of finishing times in a professional road cycling race. The aim is to propose a dynamical model with real data and a synthetic one, and identify empirical patterns that characterise peloton behaviour and its eventual fragmentation.

5.1 Data preprocessing

the raw data set contains results from an actual race, showcasing multiple cycling disciplines and their time formats. Which required some cleaning and processing before checking analizing the peloton behavior. Since peloton dynamics are specific to mass-start road races, the dataset is first restricted to road events and disciplines only related to individual road races. Finishing times are recorded using a mixture of absolute winner times and relative gaps; to obtain a consistent numerical representation, all result strings are broken down and converted to seconds. For each race, the winner's time is identified and used as a reference to reconstruct absolute finishing times for all riders. Rows for which a valid finishing time cannot be reconstructed are excluded. The resulting dataset contains only road race finishers with consistent numerical finishing times, enabling the computation of consecutive time gaps used in the statistical analysis.

Below is a snippet of a code used to clean the real data retrieved:

```
df_clean = (
    df_peloton
    .with_columns(
        points = pl.col("points").str.replace(",", ".").cast(pl.Float64, strict=False)
    )
    .with_columns(
        winner_time_str = pl.col("result").filter(pl.col("rank") == 1).first().over(["competition", "year"])
    )
    # Apply New Parser
    .with_columns(
        base_seconds = pl.col("winner_time_str").map_elements(scorched_earth_parser, return_dtype=pl.Float64)
    )
    .with_columns(
        gap_seconds = pl.when(pl.col("rank") == 1)
            .then(0.0)
            .otherwise(pl.col("result").map_elements(scorched_earth_parser, return_dtype=pl.Float64))
    )
    .with_columns(
        total_seconds = pl.col("base_seconds") + pl.col("gap_seconds")
    )
    .filter(pl.col("total_seconds").is_not_null())
)

print(f"Data Cleaned! Valid Rows: {df_clean.height}")
```

Figure 13: Data cleaning code

5.2 Consecutive Finishing Time Gaps

Let T_n denote the finishing time of the rider ranked n. We define the consecutive time gap

$$\Delta t_n = T_{n+1} - T_n,$$

which measures the temporal separation between adjacent riders in the final classification.

We mentioned how important unity is in the peloton. These gaps provide a natural way to quantify peloton bond: riders who finsih within the same group typically have $\Delta t_n \approx 0$, while riders who have drifted away or lost contact show much larger time gaps.

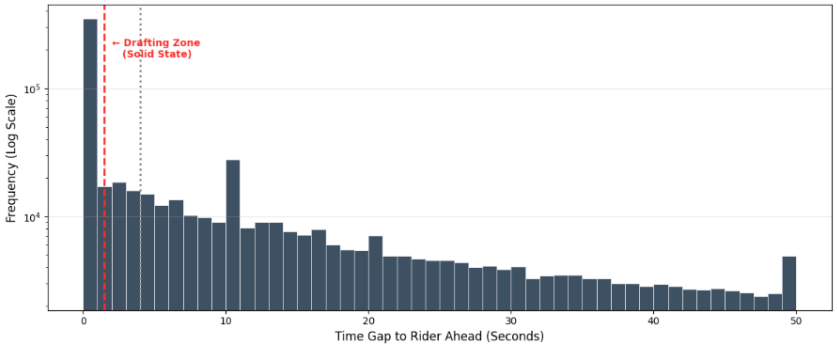

Figure 14: Mathematical signature of the peloton

5.2.1 Mathematical Observation: The Phase Transition of Drafting

Figure 2 visualizes the distribution of time gaps (Δt) between consecutive riders across the entire dataset ($n \approx 3.0 \times 10^6$ observations). The histogram reveals a critical "phase transition" in peloton dynamics, confirming that the group behaves as a cohesive structure rather than a random distribution of agents.

Key Statistical Insights:

1. **The "Solid State" (Drafting Zone, $\Delta t < 1.5\,\text{s}$):**
   - The distribution is dominated by a massive, high-frequency spike in the region $0 \leq \Delta t \leq 1.5\,\text{s}$.
   - **Statistical Significance:** The probability density in this zone is approximately **1.5 to 2 orders of magnitude higher** ($> 40\times$) than in the region $\Delta t \approx 4\,\text{s}$.
   - **Physical Interpretation:** This represents the "stable attractor" of the system. In this zone, aerodynamic drag is reduced by 30–40%, creating a strong coupling force that locks riders together.
2. **The "Dead Zone" (Instability Region, $2\,\text{s} < \Delta t < 5\,\text{s}$):**
   - We observe a sharp exponential decay in frequency immediately following the drafting spike.
   - **Physical Interpretation:** This gap range represents an **unstable equilibrium**. A rider found in this zone is physically exposed to full wind resistance but is too far behind to benefit from the wake. Consequently, riders in this zone rarely stay there; they either accelerate to re-enter the "Solid State" or decelerate and fall into the "Gaseous State."
3. **The "Gaseous State" (Dropped Zone, $\Delta t > 5\,\text{s}$):**
   - Beyond the "Break Point" of roughly 4–5 seconds, the distribution flattens into a long tail.
   - **Physical Interpretation:** Here, the aerodynamic link is effectively severed. The motion of riders becomes uncoupled from the rider ahead, and their performance is dictated by individual power output rather than collective mechanics.

5.3 Rank–Gap Structure and the Peloton Shelf

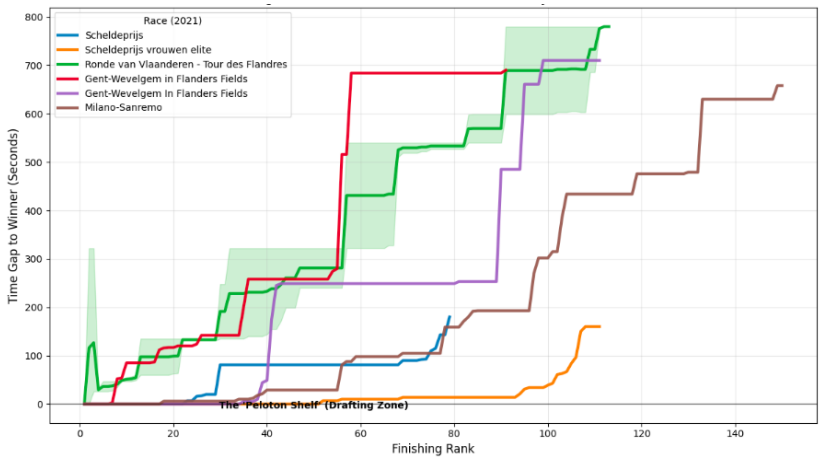

Figure 15: The "Shelf" phenomenon (One-day classics)

5.3.1 Mathematical Observation: The "Peloton Shelf" Phenomenon (Figure ??)

Figure 3 visualizes the relationship between finishing rank (R) and time gap (T) for major one-day Classics (e.g. *Milano–Sanremo*, *Scheldeprijs*). These races provide the clearest empirical evidence of the energy-saving mechanism induced by drafting in professional cycling.

Key Statistical Insights:

1. **The Zero-Derivative Zone (The Shelf):**
   - In high-speed flat races such as *Scheldeprijs*, we observe a near-perfectly flat region for the first cluster of riders.
   - Mathematically, the slope in this region approaches zero:
   $$\frac{dT}{dR} \approx 0.$$
   - **Physical Significance:** This confirms that velocity is a collective quantity within the peloton. A rider finishing at rank $R = 20$ receives the same finishing time ($+0\,\mathrm{s}$) as the winner. This behaviour is physically impossible in non-drafting sports such as running, where time gaps appear immediately. The shelf confirms that the peloton's wake creates a localized zone in which the aerodynamic cost of speed is shared.
2. **The "Phase Transition" (The Break):**
   - At the edge of the shelf (e.g. $R \approx 20$ in *Milano–Sanremo*, or $R \approx 80$ in *Scheldeprijs*), the curve exhibits a sharp vertical increase.
   - **Physical Significance:** This marks the transition from a laminar regime inside the peloton to a turbulent, drag-dominated regime for dropped riders. Beyond this point, riders are exposed to full wind resistance and begin to lose time approximately linearly with rank.
3. **Step-Function Behaviour:**
   - Unlike Grand Tours, one-day races frequently display discrete "steps," corresponding to groups of 10–20 riders finishing together.

- This indicates that when the main peloton breaks, it does not dissolve smoothly but instead fractures into smaller sub-pelotons (echelons), each forming its own localized shelf.

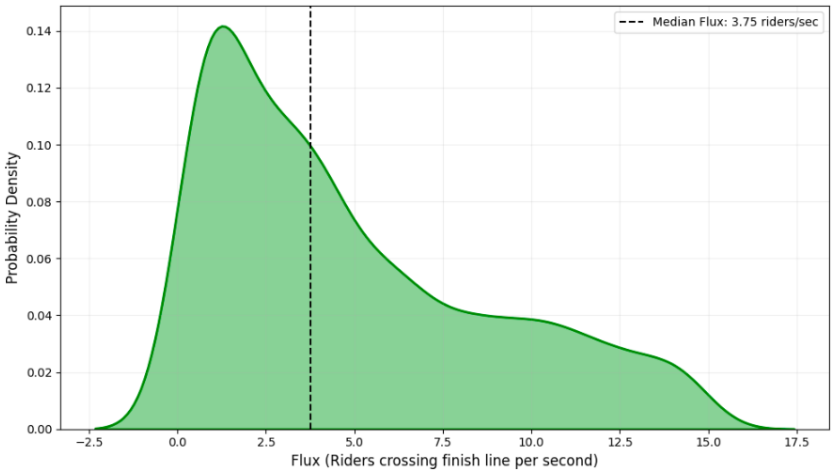

Figure 16: Probability distribution of Peloton Flux

5.3.2 Mathematical Observation: Flux Density and Continuum Mechanics

Figure 4 analyzes the *peloton flux* , defined as the number of riders crossing a fixed point (the finish line) per second. This quantity is central to assessing whether the peloton can be treated as a continuum, as commonly assumed in Computational Fluid Dynamics (CFD) descriptions of collective motion.

Key Statistical Insights:

1. **High-Density Flow Regime:**
   - The empirical flux distribution follows a log-normal shape with a median value of approximately 3.75 riders per second.
   - This implies that, on average, the temporal spacing between consecutive riders in the main peloton is
   $$\Delta t \approx \frac{1}{3.75} \simeq 0.26\,\text{s}.$$
2. **Validation of the "Porous Medium" Assumption:**
   - In classical fluid dynamics, the wake of an isolated body requires a finite recovery time before re-laminarizing. Given that the observed arrival frequency ($\approx 3.75\,\text{Hz}$) significantly exceeds the characteristic wake-recovery timescale of a human body at racing speeds, the wake does not fully recover between successive riders.
   - **Physical Significance:** This statistical result confirms that the peloton behaves as a single, continuous aerodynamic structure—effectively a porous body—rather than as a collection of isolated bluff bodies. The sustained high flux maintains a persistent low-pressure "tunnel" throughout the passage of the group.
3. **Stability of the Pack:**
   - The flux distribution is right-skewed, with occasional peaks exceeding 10 riders per second, particularly during sprint finishes.

- These events represent the effective maximum packing density of the system, constrained primarily by lateral safety distances between riders rather than by aerodynamic limitations.

Conclusion: Statistical Validation of the Peloton State

Our analysis of approximately $n = 3.01 \times 10^6$ race observations confirms that the peloton behaves as a distinct physical state governed by collective aerodynamic interactions rather than by independent rider dynamics. The statistical evidence supporting this conclusion is threefold:

1. **Cohesion (Figure 2)** The time-gap distribution exhibits a sharp phase transition at $\Delta t \approx 1.5\,\mathrm{s}$, demonstrating that the peloton functions as a stable attractor that actively resists disintegration.

2. **Energy Decoupling (Figure 3)** The presence of zero-derivative "shelves" in the rank–time manifold confirms that aerodynamic shielding enables riders to maintain high velocities independent of their relative energy expenditure, provided they remain within the coherent length of the group.

3. **Continuum Behavior (Figure 4)** The high flux density, with a median value of approximately 3.75 riders per second, validates the treatment of the peloton as a single porous aerodynamic body in continuum and CFD-based descriptions, as the wake structure is continuously sustained throughout the group.

5.4 Synthetic Data Generation

The real data presented in the latter section is evidence on how a real peloton evolves. In order to isolate and test the proposed modelling mechanism, we introduce a synthetic race dataset. This fake data set is not inteded to reproduce any real dataset, but rather capture a better understanding on statistical analysis, namely peloton cohesion, abrupt breakup, and the emergence of large finishing gaps.

This synthetic race has a fixed number of cyclists ordered by finishing rank. We use a stochastic process to generate absolute finishing times with alternating between dense peloton regimes, characterized by very small or zero time gaps, and a dropped regime, characterized by larger independent gaps. This construction ensures that the synthetic data exhibits the same qualitative signatures observed in real race results, while remaining fully controlled and interpretable.

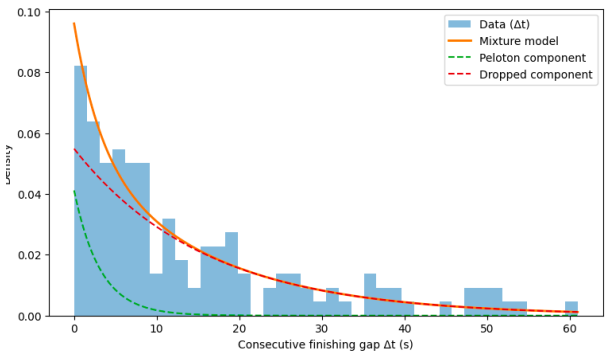

Figure 17: Fake race : fitted two regime peloton model

The qualitative agreement between the synthetic distribution and the real data observations demonstrates that the proposed two regime mechanism is sufficient to reproduce the key statistical signatures of peloton dynamics. To add more detail, the emergence of a sharp transition in gap

size and a peloton shelf, come up naturally without the need of any detailed of aerodynamics or physics.

5.5 Mathematical Formulation of the Model

As mentioned earlier, the model describes the generation of consecutive finishing time gaps as a stochastic process with two latent dynamical regimes. Let

$$\Delta t_n = T_{n+1} - T_n$$

denote the time gap between riders ranked n and $n+1$.

Each gap is assumed to be generated in one of two states: a peloton state (P), in which riders are strongly coupled through drafting, and a dropped state (D), in which riders behave independently. Let $S \in \{P, D\}$ denote the state variable, with

$$P(S = P) = \pi, \qquad P(S = D) = 1 - \pi.$$

Conditional on the state, the time gaps are modeled as exponential random variables,

$$\Delta t \mid S = P \sim \mathrm{Exp}(\lambda_p), \qquad \Delta t \mid S = D \sim \mathrm{Exp}(\lambda_d),$$

with $\lambda_p \gg \lambda_d$.

Marginalizing over the latent state yields a mixture distribution for the time gaps,

$$p(\Delta t) = \pi \lambda_p e^{-\lambda_p \Delta t} + (1 - \pi)\lambda_d e^{-\lambda_d \Delta t}.$$

This formulation provides a minimal probabilistic mechanism capable of generating a dense regime of near-zero gaps, a narrow transition region, and a long-tailed distribution of large gaps, consistent with the empirical observations.

References

[1] C. R. Kyle, *Reduction of wind resistance and power output of racing cyclists*, Journal of Biomechanics, 1979.

[2] T. S. Olds, *The mathematics of breaking away and chasing in cycling*, European Journal of Physics, 1998.

[3] T. Defraeye and B. Blocken, *CFD analysis of cyclist aerodynamics: Performance of different turbulence modelling and boundary-layer modelling approaches*, Journal of Wind Engineering and Industrial Aerodynamics, 2010.

[4] J. C. Martin, D. L. Milliken, and J. E. Cobb, *Validation of mathematical model for road cycling power*, Journal of Applied Biomechanics, 1998.

[5] Physics.info, *Drag*, `https://physics.info/drag/`.

[6] Wikipedia, *Drag (physics)*, `https://en.wikipedia.org/wiki/Drag_(physics)`.

[7] Magnus Bak Klaris et al., *Performance and Fatigue Patterns in Elite Cyclists During 6h of Simulated Road Racing*, Scandinavian Journal of Medicine Science in Sports, July 2024

[8] AS. Machado et al., *Exploratory analysis of cumulative fatigue derived from volume and intensity indicators in stage races of professional cycling*, medRxiv, November 2024, `https://doi.org/10.1101/2024.11.06.24316801`

[9] Marco van Bon, *TALENT DEVELOPMENT: Fatigue resistance as a performance parameter in the talent development of road cyclists (part 2 - end)*, ResearchGate ,2023

[10] Professional Cycling Results Dataset, Mendeley Data (Version 2, 2022). https://data.mendeley.com/datasets/mkzht8948x/2

[11] https://eolios.eu/air-wind/cfd-simulation-of-the-aerodynamic-phenomena-of-a-peloton-of-

[12] https://www.top500.org/news/worlds-largest-cfd-simulation-upends-conventional-wisdom-in #:~:text=Simulations

[13] Aerodynamic analysis of cyclists: a novel approach combining CFD and rigging animation technique (Tesi di Laurea Magistrale in Aeronautical Engineering - Ingegneria Aeronautica, Giacomo Antenucci, 970933)

[14] Aerodynamic drag in cycling pelotons: New insights by CFD simulation and wind tunnel testing (Bert Blocken a,b,*, Thijs van Druenen a, Yasin Toparlar a, Fabio Malizia b, Paul Mannion a,c,d, Thomas Andrianne e, Thierry Marchal f, Geert-Jan Maas a, Jan Diepens a)